Green's function representation for seismic interferometry by deconvolution

Kees Wapenaar*, Elmer Ruigrok, Joost van der Neut, Deyan Draganov, Jürg Hunziker, Evert Slob, Jan Thorbecke, Delft University of Technology, and Roel Snieder, Colorado School of Mines

SUMMARY

Seismic interferometry by multi-dimensional deconvolution (MDD) has recently been proposed as an alternative to the crosscorrelation method. Interferometry by MDD circumvents several of the underlying assumptions of the correlation method. We discuss a Green's function representation of the convolution type for seismic interferometry by MDD and illustrate it with a numerical example.

INTRODUCTION

Despite the strength of seismic interferometry to retrieve new seismic responses by crosscorrelating observations at different receiver locations, the method relies on a number of assumptions which are not always fulfilled in practice. Some practical circumstances that may hamper interferometry by crosscorrelation are: one-sided illumination, irregular source distribution, varying source spectra, multiples in the illuminating wave field, intrinsic losses, etc. To account for some or more of these effects, several authors have proposed interferometry by deconvolution, using a variety of approaches (Schuster and Zhou, 2006; Snieder et al., 2006; Mehta et al., 2007; Vasconcelos and Snieder, 2008; Wapenaar et al., 2008a, 2008b; van der Neut and Bakulin, 2009; Berkhout and Verschuur, 2009; van Groenestijn and Verschuur, 2010). Here we discuss a Green's function representation of the convolution type as a unifying framework for seismic interferometry by multi-dimensional deconvolution (MDD).

GREEN'S FUNCTION REPRESENTATIONS

Consider an arbitrary inhomogeneous medium with acoustic propagation velocity $c(\mathbf{x})$ and mass density $\rho(\mathbf{x})$ (where $\mathbf{x} = (x_1, x_2, x_3)$ is the Cartesian coordinate vector). In this medium we consider an arbitrary closed surface $\mathbb{S}$, with outward pointing normal vector $\mathbf{n} = (n_1, n_2, n_3)$, enclosing a volume $\mathbb{V}$. We consider two points in $\mathbb{V}$, denoted by coordinate vectors $\mathbf{x}_A$ and $\mathbf{x}_B$, see Figure 1a. We define the Fourier transform of a time-dependent function $u(t)$ as $\hat{u}(\omega) = \int_{-\infty}^{\infty} \exp(-j\omega t)u(t)\mathrm{d}t$, with j the imaginary unit and ω the angular frequency. Assuming the medium in $\mathbb{V}$ is lossless, the correlation-type representation for the acoustic Green's function between $\mathbf{x}_A$ and $\mathbf{x}_B$ in $\mathbb{V}$ reads (Wapenaar et al., 2005; van Manen et al., 2005)

$$2\Re\{\hat{G}(\mathbf{x}_B, \mathbf{x}_A, \omega)\} = \oint_{\mathbb{S}} \frac{-1}{j\omega\rho(\mathbf{x})} \Big(\partial_i \hat{G}(\mathbf{x}_B, \mathbf{x}, \omega) \hat{G}^*(\mathbf{x}_A, \mathbf{x}, \omega) - \hat{G}(\mathbf{x}_B, \mathbf{x}, \omega) \partial_i \hat{G}^*(\mathbf{x}_A, \mathbf{x}, \omega) \Big) n_i \, \mathrm{d}\mathbf{x} \quad (1)$$

(Einstein's summation convention applies to repeated lower case Latin subscripts). This representation is the basic expression for seismic interferometry (or Green's function retrieval) by crosscorrelation. The asterisk * denotes complex conjugation, hence, the products on the right-hand side correspond to crosscorrelations in the time domain of observations at two receivers at $\mathbf{x}_A$ and $\mathbf{x}_B$. Representation 1 is exact, hence, it accounts not only for the direct wave, but also for primary and multiply scattered waves.
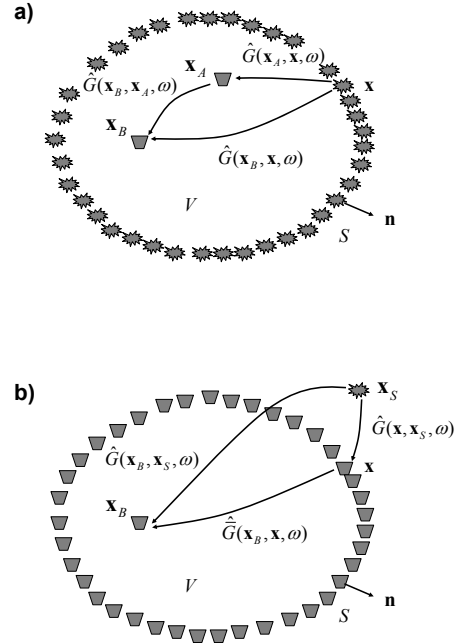

Fig. 1: *(a) Configuration for the correlation-type Green's function representation (equation 1). The medium in $\mathbb{V}$ is assumed lossless. The rays represent full responses, including primary and multiple scattering due to inhomogeneities inside as well as outside $\mathbb{S}$. (b) Configuration for the convolution-type Green's function representation (equation 2). Here the medium does not need to be lossless. The bar in $\hat{\bar{G}}$ refers to a reference state with possibly different boundary conditions at $\mathbb{S}$ and/or different medium parameters outside $\mathbb{S}$.*

Next, we consider a convolution-type representation for the Green's function. We slightly modify the configuration by taking $\mathbf{x}_A$ outside $\mathbb{S}$ and renaming it $\mathbf{x}_S$, see Figure 1b. For this configuration the convolution-type representation is given by

$$\hat{G}(\mathbf{x}_B, \mathbf{x}_S, \omega) = \oint_{\mathbb{S}} \frac{-1}{j\omega\rho(\mathbf{x})} \Big(\partial_i \hat{\bar{G}}(\mathbf{x}_B, \mathbf{x}, \omega) \hat{G}(\mathbf{x}, \mathbf{x}_S, \omega) - \hat{\bar{G}}(\mathbf{x}_B, \mathbf{x}, \omega) \partial_i \hat{G}(\mathbf{x}, \mathbf{x}_S, \omega) \Big) n_i \, \mathrm{d}\mathbf{x}. \quad (2)$$

The bar in $\hat{\bar{G}}$ is usually omitted because $\hat{G}$ and $\hat{\bar{G}}$ are usually defined in the same medium throughout space. Here the bar is introduced to denote a reference state with possibly different boundary conditions at $\mathbb{S}$ and/or different medium parameters outside $\mathbb{S}$ (but in $\mathbb{V}$ the medium parameters for $\hat{\bar{G}}$ are the same as those for $\hat{G}$). Due to the absence of

Green's function representation for interferometry by deconvolution

complex conjugation signs, the products on the right-hand side correspond to crossconvolutions in the time domain. An important difference with the correlation-type representation is that this representation remains valid in media with losses. Slob and Wapenaar (2007) use the electromagnetic equivalent of equation 2 as the starting point for interferometry by crossconvolution in lossy media. A discussion of interferometry by crossconvolution is beyond the scope of this paper. We will use equation 2 as the starting point for interferometry by deconvolution. By considering $\hat{\bar{G}}(\mathbf{x}_B, \mathbf{x}, \omega)$ under the integral as the unknown quantity, equation 2 needs to be resolved by MDD.

SIMPLIFICATION OF THE INTEGRAND

The right-hand side of equation 2 contains a combination of two convolution products. We show how we can combine these two terms into a single term. The Green's function $\hat{\bar{G}}(\mathbf{x}_B, \mathbf{x}, \omega)$ under the integral is the unknown that we want to resolve by MDD. The Green's function $\hat{G}(\mathbf{x}_B, \mathbf{x}_S, \omega)$ on the left-hand side and $\hat{G}(\mathbf{x}, \mathbf{x}_S, \omega)$ under the integral are related to the observations. Hence, $\hat{G}$ is defined in the actual medium inside as well as outside $\mathbb{S}$, but for $\hat{\bar{G}}$ we are free to choose convenient boundary conditions at $\mathbb{S}$. In the following we let $\mathbb{S}$ be an absorbing boundary for $\hat{\bar{G}}(\mathbf{x}_B, \mathbf{x}, \omega)$. Furthermore, we write $\hat{G}(\mathbf{x}, \mathbf{x}_S, \omega)$ as the superposition of an inward and outward propagating field at $\mathbf{x}$ on $\mathbb{S}$, according to $\hat{G} = \hat{G}^{\mathrm{in}} + \hat{G}^{\mathrm{out}}$. In the high-frequency regime, the derivatives are approximated by multiplying each constituent (direct wave, scattered wave, etc.) with $\pm jk |\cos \alpha|$, where $k = \omega/c$ and α is the angle between the relevant ray and the normal on $\mathbb{S}$. The main contributions come from stationary points on $\mathbb{S}$. At those points the ray angles for $\hat{G}$ and $\hat{\bar{G}}$ are identical. However, the stationary points are different for terms containing $\hat{G}^{\mathrm{in}}$ than for those containing $\hat{G}^{\mathrm{out}}$. For terms containing $\hat{G}^{\mathrm{in}}$ we have at the stationary points

$$\left((\partial_i \hat{\bar{G}}) \hat{G}^{\mathrm{in}} - \hat{\bar{G}}(\partial_i \hat{G}^{\mathrm{in}}) \right) n_i \approx \tag{3}$$
$$-jk |\cos \alpha| \left(\hat{\bar{G}} \hat{G}^{\mathrm{in}} - \hat{\bar{G}}(-\hat{G}^{\mathrm{in}}) \right) =$$
$$-2jk |\cos \alpha| \hat{\bar{G}} \hat{G}^{\mathrm{in}} \approx 2(n_i \partial_i \hat{\bar{G}}) \hat{G}^{\mathrm{in}},$$

whereas for terms containing $\hat{G}^{\mathrm{out}}$ we have

$$\left((\partial_i \hat{\bar{G}}) \hat{G}^{\mathrm{out}} - \hat{\bar{G}}(\partial_i \hat{G}^{\mathrm{out}}) \right) n_i \approx \tag{4}$$
$$-jk |\cos \alpha| \left(\hat{\bar{G}} \hat{G}^{\mathrm{out}} - \hat{\bar{G}} \hat{G}^{\mathrm{out}} \right) = 0.$$

Using equations 3 and 4 in equation 2, and rewriting $\mathbf{x}$ as $\mathbf{x}_A$ (standing for a receiver coordinate vector), we obtain

$$\hat{G}(\mathbf{x}_B, \mathbf{x}_S, \omega) = \tag{5}$$
$$\oint_{\mathbb{S}_{\mathrm{rec}}} \frac{-2}{j\omega\rho(\mathbf{x}_A)} \left(n_i \partial_i^A \hat{\bar{G}}(\mathbf{x}_B, \mathbf{x}_A, \omega) \right) \hat{G}^{\mathrm{in}}(\mathbf{x}_A, \mathbf{x}_S, \omega) \, \mathrm{d}\mathbf{x}_A.$$

We added a subscript 'rec' in $\mathbb{S}_{\mathrm{rec}}$ to denote that the integration surface contains the receivers of the Green's function $\hat{G}^{\mathrm{in}}$. The superscript A in ∂_i^A denotes that the differentiation is carried out with respect to the components of $\mathbf{x}_A$, hence, this operation turns the monopole response $\hat{\bar{G}}(\mathbf{x}_B, \mathbf{x}_A, \omega)$ into a dipole response. For convenience we introduce a dipole Green's function as

$$\hat{\bar{G}}_{\mathrm{d}}(\mathbf{x}_B, \mathbf{x}_A, \omega) = \frac{-2}{j\omega\rho(\mathbf{x}_A)} \left(n_i \partial_i^A \hat{\bar{G}}(\mathbf{x}_B, \mathbf{x}_A, \omega) \right), \tag{6}$$

so that equation 5 simplifies to

$$\hat{G}(\mathbf{x}_B, \mathbf{x}_S, \omega) = \oint_{\mathbb{S}_{\mathrm{rec}}} \hat{\bar{G}}_{\mathrm{d}}(\mathbf{x}_B, \mathbf{x}_A, \omega) \hat{G}^{\mathrm{in}}(\mathbf{x}_A, \mathbf{x}_S, \omega) \, \mathrm{d}\mathbf{x}_A. \tag{7}$$

In the underlying representation (equation 2) it was assumed that $\mathbf{x}_B$ lies in $\mathbb{V}$. In several applications of MDD $\mathbf{x}_B$ is a receiver on $\mathbb{S}_{\mathrm{rec}}$. For those applications we take $\mathbf{x}_B$ just inside $\mathbb{S}_{\mathrm{rec}}$ to avoid several subtleties of taking $\mathbf{x}_B$ on $\mathbb{S}_{\mathrm{rec}}$. In those applications it is often useful to consider only the outward propagating part of the wave field at $\mathbf{x}_B$. Applying decomposition at both sides of equation 7 gives

$$\hat{G}^{\mathrm{out}}(\mathbf{x}_B, \mathbf{x}_S, \omega) = \oint_{\mathbb{S}_{\mathrm{rec}}} \hat{\bar{G}}_{\mathrm{d}}^{\mathrm{out}}(\mathbf{x}_B, \mathbf{x}_A, \omega) \hat{G}^{\mathrm{in}}(\mathbf{x}_A, \mathbf{x}_S, \omega) \, \mathrm{d}\mathbf{x}_A. \tag{8}$$

Equation 8 is nearly the same (except for a different normalization) as our previously derived one-way representation for MDD (Wapenaar et al., 2008a). In the following we continue with equation 7. In most practical situations receivers are not available on a closed boundary, so the integration in equation 7 is necessarily restricted to an open receiver boundary $\mathbb{S}_{\mathrm{rec}}$. When the sources are located on one side of $\mathbb{S}_{\mathrm{rec}}$ (outside $\mathbb{V}$), then it suffices to take the integral over this open receiver boundary: since the underlying representation (equation 2) is of the convolution type, radiation conditions apply on the half-sphere that closes the boundary (assuming the half-sphere boundary is absorbing and its radius is sufficiently large), meaning that the contribution of the integral over that half-sphere vanishes. Hence, in the following we replace the closed boundary integral by an open boundary integral. In the time domain equation 7 thus becomes

$$G(\mathbf{x}_B, \mathbf{x}_S, t) = \int_{\mathbb{S}_{\mathrm{rec}}} \bar{G}_{\mathrm{d}}(\mathbf{x}_B, \mathbf{x}_A, t) * G^{\mathrm{in}}(\mathbf{x}_A, \mathbf{x}_S, t) \, \mathrm{d}\mathbf{x}_A, \tag{9}$$

where the asterisk $*$ denotes temporal convolution. This is an implicit representation of the convolution type for $\bar{G}_{\mathrm{d}}(\mathbf{x}_B, \mathbf{x}_A, t)$. If it were a single equation, the inverse problem would be ill-posed. However, equation 9 exists for each source position $\mathbf{x}_S$, which we will denote from hereon by $\mathbf{x}_S^{(i)}$, where i denotes the source number. Solving the ensemble of equations for $\bar{G}_{\mathrm{d}}(\mathbf{x}_B, \mathbf{x}_A, t)$ involves MDD.

TRANSIENT SOURCES

For practical applications the Green's functions G and G^{in} in equation 9 should be replaced by responses of real sources, i.e., Green's functions convolved with source functions. For transient sources we write for the responses at $\mathbf{x}_A$ and $\mathbf{x}_B$

$$u^{\mathrm{in}}(\mathbf{x}_A, \mathbf{x}_S^{(i)}, t) = G^{\mathrm{in}}(\mathbf{x}_A, \mathbf{x}_S^{(i)}, t) * s^{(i)}(t), \tag{10}$$
$$u(\mathbf{x}_B, \mathbf{x}_S^{(i)}, t) = G(\mathbf{x}_B, \mathbf{x}_S^{(i)}, t) * s^{(i)}(t). \tag{11}$$

Convolving both sides of equation 9 with $s^{(i)}(t)$ we obtain

$$u(\mathbf{x}_B, \mathbf{x}_S^{(i)}, t) = \int_{\mathbb{S}_{\mathrm{rec}}} \bar{G}_{\mathrm{d}}(\mathbf{x}_B, \mathbf{x}_A, t) * u^{\mathrm{in}}(\mathbf{x}_A, \mathbf{x}_S^{(i)}, t) \, \mathrm{d}\mathbf{x}_A. \tag{12}$$

Equation 12 is illustrated in Figure 2a for the situation of direct-wave interferometry and in Figure 2b for reflected-wave interferometry (with superscripts 'out' added).
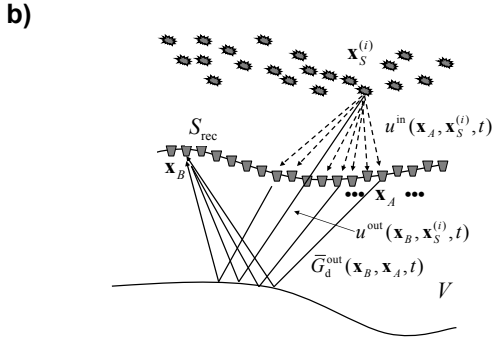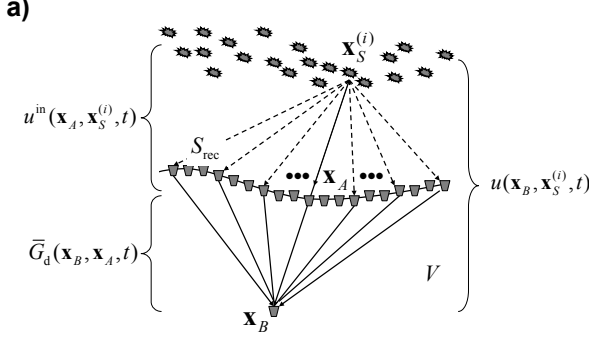
a)

b)

Fig. 2: *(a) Illustration of the convolutional model (equation 12), underlying interferometry by MDD for the situation of direct-wave interferometry. (b) Idem, for reflected-wave interferometry.*

RELATION WITH THE CORRELATION METHOD

To make the relation with the correlation method more transparent, we crosscorrelate both sides of equation 12 with $u^{\mathrm{in}}(\mathbf{x}'_A, \mathbf{x}^{(i)}_S, t)$ (with $\mathbf{x}'_A$ on $\mathbb{S}_{\mathrm{rec}}$) and take the sum over all sources, as proposed by van der Neut et al. (2010). This gives

$$C(\mathbf{x}_B, \mathbf{x}'_A, t) = \int_{\mathbb{S}_{\mathrm{rec}}} \bar{G}_{\mathrm{d}}(\mathbf{x}_B, \mathbf{x}_A, t) * \Gamma(\mathbf{x}_A, \mathbf{x}'_A, t) \, \mathrm{d}\mathbf{x}_A, \quad (13)$$

where

$$C(\mathbf{x}_B, \mathbf{x}'_A, t) \qquad\qquad (14)$$
$$= \sum_i u(\mathbf{x}_B, \mathbf{x}^{(i)}_S, t) * u^{\mathrm{in}}(\mathbf{x}'_A, \mathbf{x}^{(i)}_S, -t)$$
$$= \sum_i G(\mathbf{x}_B, \mathbf{x}^{(i)}_S, t) * G^{\mathrm{in}}(\mathbf{x}'_A, \mathbf{x}^{(i)}_S, -t) * S^{(i)}(t),$$

$$\Gamma(\mathbf{x}_A, \mathbf{x}'_A, t) \qquad\qquad (15)$$
$$= \sum_i u^{\mathrm{in}}(\mathbf{x}_A, \mathbf{x}^{(i)}_S, t) * u^{\mathrm{in}}(\mathbf{x}'_A, \mathbf{x}^{(i)}_S, -t)$$
$$= \sum_i G^{\mathrm{in}}(\mathbf{x}_A, \mathbf{x}^{(i)}_S, t) * G^{\mathrm{in}}(\mathbf{x}'_A, \mathbf{x}^{(i)}_S, -t) * S^{(i)}(t),$$

with

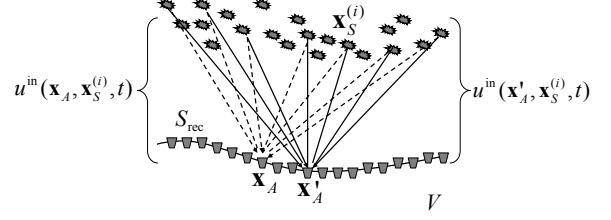$$S^{(i)}(t) = s^{(i)}(t) * s^{(i)}(-t). \qquad\qquad (16)$$

Fig. 3: *Fields involved in the illumination function $\Gamma(\mathbf{x}_A, \mathbf{x}'_A, t)$ (equation 15).*

The correlation function $C(\mathbf{x}_B, \mathbf{x}'_A, t)$ defined in equation 14 is the traditional interferometry relation (for example as employed in the virtual source method of Bakulin and Calvert (2006)). Equation 13 shows that this correlation function is proportional to the Green's function $\bar{G}_{\mathrm{d}}(\mathbf{x}_B, \mathbf{x}_A, t)$, smeared in space and time by $\Gamma(\mathbf{x}_A, \mathbf{x}'_A, t)$. According to equation 15, $\Gamma(\mathbf{x}_A, \mathbf{x}'_A, t)$ is the crosscorrelation of the inward propagating wave fields at $\mathbf{x}_A$ and $\mathbf{x}'_A$, summed over the sources, see Figure 3. We call $\Gamma(\mathbf{x}_A, \mathbf{x}'_A, t)$ the illumination function (van der Neut et al., 2010). If we would have a regular distribution of sources with equal autocorrelation functions $S(t)$ along a large source boundary, and if the medium between the source and receiver boundaries was homogeneous and lossless, the illumination function would approach $\Gamma(\mathbf{x}_A, \mathbf{x}'_A, t) \approx (\rho c/2)^2 \delta(\mathbf{x}_A - \mathbf{x}'_A)S(t)$ [here $\delta(\mathbf{x}_A - \mathbf{x}'_A)$ is defined for $\mathbf{x}_A$ and $\mathbf{x}'_A$ both on $\mathbb{S}_{\mathrm{rec}}$; the approximation sign accounts for the fact that in reality the illumination function is spatially band-limited because the correlation in equation 15 does not compensate for evanescent waves]. Hence, for this situation, equation 13 would simplify to $C(\mathbf{x}_B, \mathbf{x}'_A, t) \approx (\rho c/2)^2 \bar{G}_{\mathrm{d}}(\mathbf{x}_B, \mathbf{x}'_A, t) * S(t)$, so the Green's function $\bar{G}_{\mathrm{d}}(\mathbf{x}_B, \mathbf{x}'_A, t)$ could be simply obtained by deconvolving the correlation function $C(\mathbf{x}_B, \mathbf{x}'_A, t)$ for $S(t)$. In practice, there are many factors that make the illumination function $\Gamma(\mathbf{x}_A, \mathbf{x}'_A, t)$ deviate from a spatial delta function. Among these factors are the irregularity of the source distribution (Wapenaar et al., 2008b; van der Neut et al., 2010), medium inhomogeneities (van der Neut and Bakulin, 2009), a finite aperture (Schuster and Zhou, 2006), asymmetric illumination of saltflanks (van der Neut and Thorbecke, 2009) or of inter-well reflectors (Minato et al., 2009), multiple reflections in the illuminating wavefield (Wapenaar and Verschuur, 1996; Amundsen, 1999), intrinsic losses (Slob et al., 2007; Hunziker et al., 2009; Fan et al., 2009), etc. In all those cases equation 13 needs to be inverted by MDD, i.e., the effects of the illumination function $\Gamma(\mathbf{x}_A, \mathbf{x}'_A, t)$ need to be removed from the correlation function $C(\mathbf{x}_B, \mathbf{x}'_A, t)$ to obtain the Green's function $\bar{G}_{\mathrm{d}}(\mathbf{x}_B, \mathbf{x}_A, t)$.

This is illustrated with a numerical example in Figure 4. The North-South array in central USA in Figure 4a represents $\mathbb{S}_{\mathrm{rec}}$, the East-West array a number of $\mathbf{x}_B$ positions, and the blue dots along the East coast represent an irregular distribution of source positions $\mathbf{x}^{(i)}_S$. Figure 4b is the illumination function $\Gamma(\mathbf{x}_A, \mathbf{x}'_A, t)$ for fixed $\mathbf{x}'_A$ (the red dot in Figure 4a) and variable $\mathbf{x}_A$ (the North-South array in Figure 4a). Figures 4c and d show in red the correlation function $C(\mathbf{x}_B, \mathbf{x}'_A, t)$ and the deconvolution result $\bar{G}_{\mathrm{d}}(\mathbf{x}_B, \mathbf{x}'_A, t)$, respectively, for fixed $\mathbf{x}'_A$ (the red dot) and variable $\mathbf{x}_B$ (the East-West array in Figure 4a). The obtained Green's function $\bar{G}_{\mathrm{d}}(\mathbf{x}_B, \mathbf{x}'_A, t)$ matches

Green's function representation for interferometry by deconvolution

the reference solution (in black) significantly better than the correlation function.

Note that the illumination function plays a similar role in interferometry by MDD as the point-spread function (or spatial resolution function) in seismic migration (Schuster and Hu, 2000; Gelius et al., 2002). The point-spread function is defined as the migration result of the response of a single point scatterer and as such is a useful tool to asses migration results in relation with geological parameters, background model, acquisition parameters, etc. Moreover, it is sometimes used in migration deconvolution to improve the spatial resolution (Hu et al., 2001). An important difference is that the illumination function is obtained from measured responses whereas the point-spread function is modeled in a background medium. As a result, the illumination function accounts much more accurately for the distorting effects of the medium inhomogeneities, including multiple scattering.

NOISE SOURCES

We show that equation 13 also holds for the situation of simultaneously acting uncorrelated noise sources. To this end, we define the correlation function and the illumination function, respectively, as

$$C(\mathbf{x}_B, \mathbf{x}'_A, t) = \langle u(\mathbf{x}_B, t) * u^{\text{in}}(\mathbf{x}'_A, -t) \rangle, \quad (17)$$

$$\Gamma(\mathbf{x}_A, \mathbf{x}'_A, t) = \langle u^{\text{in}}(\mathbf{x}_A, t) * u^{\text{in}}(\mathbf{x}'_A, -t) \rangle, \quad (18)$$

where the noise responses are defined as

$$u^{\text{in}}(\mathbf{x}'_A, t) = \sum_i G^{\text{in}}(\mathbf{x}'_A, \mathbf{x}_S^{(i)}, t) * N^{(i)}(t), \quad (19)$$

$$u^{\text{in}}(\mathbf{x}_A, t) = \sum_j G^{\text{in}}(\mathbf{x}_A, \mathbf{x}_S^{(j)}, t) * N^{(j)}(t), \quad (20)$$

$$u(\mathbf{x}_B, t) = \sum_j G(\mathbf{x}_B, \mathbf{x}_S^{(j)}, t) * N^{(j)}(t), \quad (21)$$

and where the noise signals are mutually uncorrelated, according to

$$\langle N^{(j)}(t) * N^{(i)}(-t) \rangle = \delta_{ij} S^{(i)}(t). \quad (22)$$

Upon substitution of equations $19 - 21$ into equations 17 and 18, using equation 22, it follows that the correlation function and the illumination function as defined in equations 17 and 18 are identical to those defined in equations 14 and 15. Hence, whether we consider transient or noise sources, equation 13 is the relation that needs to be inverted by MDD to resolve the Green's function $\bar{G}_d(\mathbf{x}_B, \mathbf{x}_A, t)$. It is beyond the scope of this paper to discuss the numerical aspects of this inversion.

CONCLUSIONS

We have derived a Green's function representation for seismic interferometry by MDD. It appears that the correlation function, used in correlation interferometry, can be written as the true Green's function, smeared in space and time by an illumination function. Similar as the correlation function, the illumination function is obtained directly from the measured data. Interferometry by MDD removes the illumination function from the correlation function and thus compensates for the effects of one-sided illumination, irregular source distribution, intrinsic losses, etc. The theory discussed here covers most of the configurations usually considered, except that for passive reflected-wave interferometry some modifications are required, see van der Neut et al. (2010) for a further discussion.
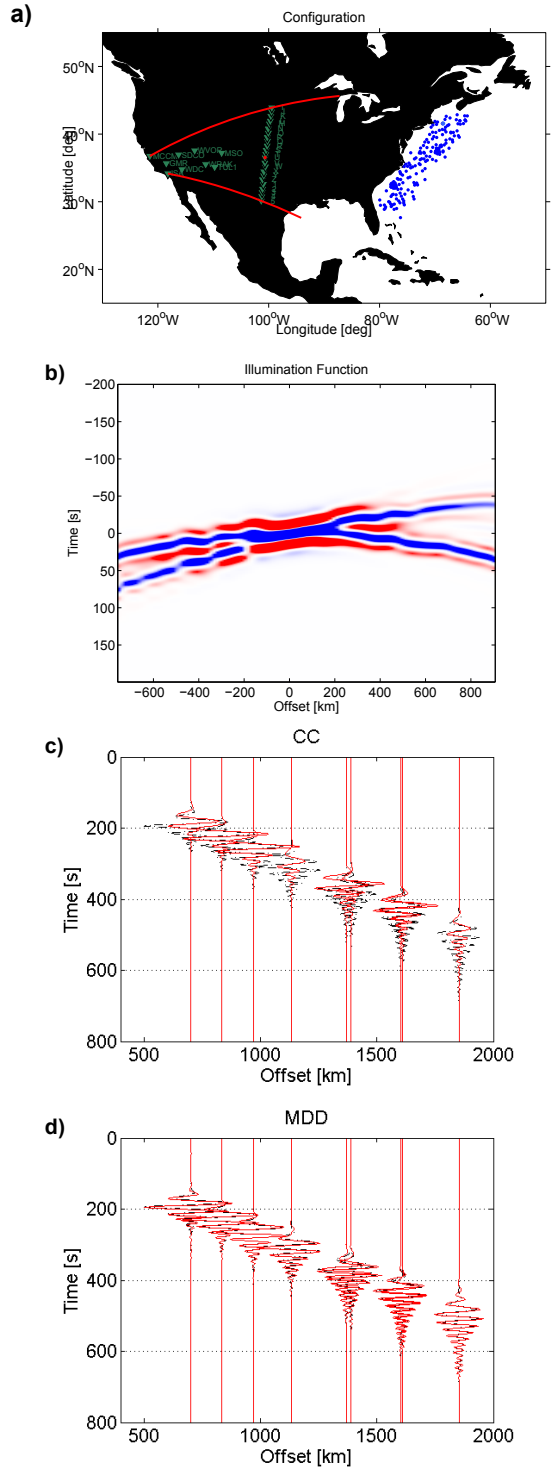

Fig. 4: *Illustration of interferometry by MDD for surface waves. (a) Configuration. (b) Illumination function. (c) Crosscorrelation result (red) compared with reference solution (black). (d) MDD result.*

Green's function representation for interferometry by deconvolution

References

Amundsen, L., 1999, Elimination of free surface-related multiples without need of the source wavelet: 69th Annual International SEG Meeting, Expanded Abstracts, 1064–1067.

Bakulin, A. and R. Calvert, 2006, The virtual source method: Theory and case study: Geophysics, **71**, SI139–SI150.

Berkhout, A. J. and D. J. Verschuur, 2009, Integrated imaging with active and passive seismic data: 79th Annual International SEG Meeting, Expanded Abstracts, 1592–1596.

Fan, Y., R. Snieder, and J. Singer, 2009, 3-D controlled source electromagnetic (CSEM) interferometry by multi-dimensional deconvolution: 79th Annual International SEG Meeting, Expanded Abstracts, 779–784.

Gelius, L.-J., I. Lecomte, and H. Tabti, 2002, Analysis of the resolution function in seismic prestack depth imaging: Geophysical Prospecting, **50**, 505–515.

Hu, J., G. T. Schuster, and P. Valasek, 2001, Poststack migration deconvolution: Geophysics, **66**, 939–952.

Hunziker, J., E. Slob, and K. Wapenaar, 2009, Controlled source electromagnetic interferometry by multidimensional deconvolution: spatial sampling aspects: 71rst Annual International EAGE Meeting, Expanded Abstracts, P074.

Mehta, K., R. Snieder, and V. Graizer, 2007, Extraction of near-surface properties for a lossy layered medium using the propagator matrix: Geophysical Journal International, **169**, 271–280.

Minato, S., T. Matsuoka, T. Tsuji, D. Draganov, J. Hunziker, and K. Wapenaar, 2009, Application of seismic interferometry by multidimensional deconvolution to crosswell seismic reflection using singular-value decomposition: 79th Annual International SEG Meeting, Expanded Abstracts, 1688–1692.

Schuster, G. T. and J. Hu, 2000, Green's function for migration: Continuous recording geometry: Geophysics, **65**, 167–175.

Schuster, G. T. and M. Zhou, 2006, A theoretical overview of model-based and correlation-based redatuming methods: Geophysics, **71**, SI103–SI110.

Slob, E. and K. Wapenaar, 2007, GPR without a source: Cross-correlation and cross-convolution methods: IEEE Transactions on Geoscience and Remote Sensing, **45**, 2501–2510.

Slob, E., K. Wapenaar, and R. Snieder, 2007, Interferometry in dissipative media: Adressing the shallow sea problem for Seabed Logging applications: 77th Annual International SEG Meeting, Expanded Abstracts, 559–563.

Snieder, R., J. Sheiman, and R. Calvert, 2006, Equivalence of the virtual-source method and wave-field deconvolution in seismic interferometry: Physical Review E, **73**, 066620–1–066620–9.

van der Neut, J. and A. Bakulin, 2009, Estimating and correcting the amplitude radiation pattern of a virtual source: Geophysics, **74**, SI27–SI36.

van der Neut, J., E. Ruigrok, D. Draganov, and K. Wapenaar, 2010, Retrieving the earth's reflection response by multi-dimensional deconvolution of ambient seismic noise: 72nd Annual International EAGE Meeting, Expanded Abstracts, P406.

van der Neut, J. and J. Thorbecke, 2009, Resolution function for controlled-source seismic interferometry: a data-driven diagnosis: 79th Annual International SEG Meeting, Expanded Abstracts, 4090–4094.

van Groenestijn, G. J. A. and D. J. Verschuur, 2010, Estimation of primaries by sparse inversion from passive seismic data: Geophysics, **75**, (in press).

van Manen, D.-J., J. O. A. Robertsson, and A. Curtis, 2005, Modeling of wave propagation in inhomogeneous media: Physical Review Letters, **94**, 164301–1–164301–4.

Vasconcelos, I. and R. Snieder, 2008, Interferometry by deconvolution: Part 1 - Theory for acoustic waves and numerical examples: Geophysics, **73**, S115–S128.

Wapenaar, C. P. A. and D. J. Verschuur, 1996, Processing of ocean bottom data: Presented at the The Delphi Acquisition Project, Volume I, Delft University of Technology.

Wapenaar, K., J. Fokkema, and R. Snieder, 2005, Retrieving the Green's function in an open system by cross-correlation: a comparison of approaches (L): Journal of the Acoustical Society of America, **118**, 2783–2786.

Wapenaar, K., E. Slob, and R. Snieder, 2008a, Seismic and electromagnetic controlled-source interferometry in dissipative media: Geophysical Prospecting, **56**, 419–434.

Wapenaar, K., J. van der Neut, and E. Ruigrok, 2008b, Passive seismic interferometry by multi-dimensional deconvolution: Geophysics, **73**, A51–A56.